Environmental Science & Technology

ARTICLE

pubs.acs.org/est

Case Study of Water-Soluble Metal Containing Organic Constituents of Biomass Burning Aerosol

Alexandra L. Chang-Graham,[†] Luisa T. M. Profeta,[‡] Timothy J. Johnson,[†] Robert J. Yokelson,[∥] Alexander Laskin,[*,§] and Julia Laskin[*,†]

[†]Chemical and Materials Sciences Division, [‡]National Security Division, [§]William R. Wiley Environmental and Molecular Sciences Laboratory, Pacific Northwest National Laboratory, P.O. Box 999, MSIN K8-88, Richland, Washington 99352, United States

[∥]Department of Chemistry, University of Montana, Missoula, Montana 59812, United States

Supporting Information

ABSTRACT: Natural and prescribed biomass fires are a major source of aerosols that may persist in the atmosphere for several weeks. Biomass burning aerosols (BBA) can be associated with long-range transport of water-soluble N-, S-, P-, and metal-containing species. In this study, BBA samples were collected using a particle-into-liquid sampler (PILS) from laboratory burns of vegetation collected on military bases in the southeastern and southwestern United States. The samples were then analyzed using high resolution electrospray ionization mass spectrometry (ESI/HR-MS) that enabled accurate mass measurements for hundreds of species with m/z values between 70 and 1000 and assignment of elemental formulas. Mg, Al, Ca, Cr, Mn, Fe, Ni, Cu, Zn, and Ba-containing organometallic species were identified. The results suggest that the biomass may have accumulated metal-containing species that were re-emitted during biomass burning. Further research into the sources, dispersion, and persistence of metal-containing aerosols, as well as their environmental effects, is needed.

INTRODUCTION

Biomass burning is by far the largest source of primary, fine organic aerosols in the atmosphere.[1] These large quantities of organic aerosol can persist in the atmosphere for several weeks and be transported over long distances. As a result, biomass burning aerosol (BBA) has significant impacts on climate via interaction with solar radiation and modifications of clouds. BBA may also significantly affect air quality and human health. Identifying the chemical composition of BBA is one step toward understanding their short- and long-term effects on atmospheric and aquatic ecosystems, climate, and human health.

A significant fraction (45−75%) of the organic matter in BBA is water-soluble organic carbon (WSOC).[2,3] WSOC is commonly found in particles internally mixed with inorganic species, and it may affect the particles' hygroscopic properties and ability to act as cloud condensation nuclei (CCN). Specifically, WSOC may enhance the CCN activity of organic-laden particles by increasing their solubility[4,5] or by reducing the surface tension of nucleating droplets thereby altering the condensation rate of water molecules.[6] Furthermore, absorption of visible and UV light by WSOC constituents of smoke particles, including those dissolved in cloud droplets, contributes to the positive radiative forcing of climate.[7,8]

Transport and deposition of the organic particulate matter has further effects on the atmosphere, the global carbon and nitrogen cycles, and climate. Global dry and wet deposition of aerosol organic carbon (OC) is estimated to be 11 Tg C y^{-1} and 47 Tg C y^{-1}, respectively.[9] Deposition of water-soluble organic carbon (WSOC) and nitrogen (WSON) from atmospheric particles has a profound effect on the organic carbon and nitrogen concentration in aquatic and terrestrial ecosystems.[10] Moreover, long-range transport of OC in particles contributes to redistribution of organic material at both the regional and global scale. It follows that detailed characterization of the composition of aerosol WSOC/N is important for understanding the effects of atmospheric aerosols on the carbon and nitrogen biogeochemical cycling between the atmosphere, soil, and water.

Natural and industrial processes such as mining, refining, agriculture,[11] waste incineration,[12] and military operations[13] can all introduce metals such as Zn, Pb, Ni, Cu, Cr, and Fe into terrestrial and aquatic ecosystems. Plants can uptake metal pollutants from contaminated soil and water.[14] Plant bark and leaves can also accumulate metals through both wet and dry deposition of metal-containing aerosols (MCA).[15] Burning the affected biomass can then result in the release of metal-containing compounds including salts, oxides, and organometallic complexes that affect multiphase aerosol chemistry, particle optical properties, phase partitioning, and solubilization of metals in fog and cloudwater.[16]

Understanding the environmental impact of BBA is furthered by fundamental knowledge of the relationship between their composition and the physicochemical properties. High-resolution mass spectrometry (HR-MS) coupled with soft ionization techniques such as electrospray (ESI) is a powerful technique for structural characterization of molecules in complex mixtures such as WSOC/N.[17] We recently reported detailed characterization of the organic compounds in BBA emitted from laboratory burns of different biomass materials.[18,19] We showed that a variety of

Received: September 2, 2010
Accepted: December 17, 2010
Revised: November 15, 2010
Published: January 10, 2011

oxygenated organic compounds and nitrogen-containing compounds account for a significant fraction of the organic material in BBA.[18,19] We further demonstrated that ESI/HR-MS is a unique tool for comprehensive chemical characterization of WSOC/N in aerosol. Those studies employed collection of particles on substrates followed by solvent extraction using organic/water solvents prior to ESI/HR-MS analysis. Analysis of WSOC/N compounds requires extraction of BBA samples into water, which is often not very efficient because a substantial fraction of water-soluble compounds , in bulk samples, may be covered with nonsoluble organic resins present in BBA.[20]

Efficient extraction of water-soluble constituents of aerosol can be accomplished using a particle-into-liquid-sampler (PILS).[21] PILS collection employs rapid growth of individual particles into aqueous microdroplets that are subsequently impacted onto a surface covered with a layer of flowing water. The flowing water transfers the resulting aqueous extracts from the impactor to collection vials. PILS is most commonly used for collection and analysis of inorganic components of aerosols that are subsequently quantified using online ion chromatography (IC).[22] More recently, PILS has been utilized for the analysis of total WSOC concentrations using an online total carbon analyzer[23,24] as well as for off-line ESI-MS and GC-MS analyses of aerosol extracts collected in vials.[20,25]

In this study we utilized PILS sample collection followed by ESI/HR-MS analysis for molecular characterization of WSOC in BBA emitted by laboratory burns of biomass fuels collected at military bases in the southeastern and southwestern U.S. A variety of water-soluble nitrogen- and metal-containing organic compounds containing both alkaline earth metals such as Ca, Ba, and Mg and transition metals such as Mn, Fe, Ni, Cu, and Zn were identified. Many of the identified compounds had not been detected in our previous studies of BBA using similar techniques.[18−20] The presence of these compounds could be due to a number of reasons: (1) different vegetation burned, (2) different extraction methodology, and (3) different land-use on or near the sites. It is likely that additional research could identify marker species associated with the specific reasons given above. This would be of value because transition metals and their complexes play an important role in the atmospheric chemistry of cloud, fog, rain, and snow.[16] Concentrations of metals in ambient aerosol in areas impacted by prescribed burns reported in the literature span the range between 10 and 30 ng/m^3 (Ca, Mn, Cu) to 150−300 ng/m^3 (Fe, Zn).[26] It is difficult to quantify water-soluble metals-containing species in aerosols, but a recent study by Oakes et al. reported water-soluble Fe(II) at ∼100 ng/m^3 in BBA and up to ∼100 ng/m^3 in urban aerosol.[27] However, a substantial presence of different metal-containing organic compounds in BBA has not been previously reported.

EXPERIMENTAL SECTION

Biomass fuel samples consisting of leaves, needles, and branches were collected from three U.S. military bases: Vandenberg Air Force Base, CA; Fort Benning, GA; and Marine Corps Base Camp Lejeune, NC. The BBA samples described in this manuscript are summarized in Table 1 and were collected during lab burns of Vandenberg manzanita (VM), or sage (VS), Ft. Benning pine litter (FB), and assorted hardwood species from Camp Lejeune reflecting one, two, or over ten years regrowth (L1, L2, L10) since the last mechanical clearing or burn. The burns were performed in the U.S. Forest Service Fire Science Laboratory (Missoula, MT) in February 2009. More detailed descriptions of the biomass fuel, test facility setup, and the logistics of the experiment can be found elsewhere.[28]

Water extracts of BBA samples were collected using a PILS at an air sample flow rate of 15 slpm and a liquid wash water flow rate of 100 μL/min. The collection time was 5 min per individual vial corresponding to extraction of the BBA material sampled out of 75 L of air into 0.5 mL of water. Three to five vials of WSOC samples were collected during each burn. Background samples were collected by sampling air through a high efficiency particulate air filter (HEPA). Previous studies indicated that the organic content of BBA was highest when smoldering combustion of biomass was producing a dense white to brownish smoke.[29] After examining the videos recorded during the experiments, we selected PILS samples collected during the smoldering phases of 6 burns as listed in Table 1.

The samples were analyzed using a high-resolution LTQ-Orbitrap mass spectrometer (Thermo Electron, Inc.) equipped with an electrospray ionization (ESI) source. Samples were injected through a pulled fused silica capillary (50 μm ID) at a flow rate of 0.4−0.6 μL/min and a spray voltage of 3.5−4.5 kV. Positive and negative mode spectra were acquired over an m/z range of 70−2000 with a resolving power of 60,000 ($m/\Delta m$) at 400 m/z. Because negative mode ESI/MS spectra were indistinguishable from the background we limit our discussion to BBA constituents detected in the positive mode.

Several experiments were performed to determine the best approach for acquiring ESI/HR-MS spectra of PILS-collected BBA extracts. The samples produced mass spectra with the highest intensity peaks when the original PILS-collected extracts were injected directly, without any pretreatment. Adding methanol, acetonitrile, or trifluoroacetic acid to samples did not result in improved ion signal. Based on these observations, no additional sample preparation was performed prior to the analysis.

MS peaks with a signal-to-noise ratio greater than 3 were extracted from raw spectra using Decon2LS and subsequently clustered using the VIPER program (http://ncrr.pnl.gov/software/). Clustering of mass spectra aligns signal intensities observed in experimental spectra along a common m/z axis within a specified tolerance to facilitate peak identification and comparison of spectral data obtained for different samples or settings. Clustering was performed using a mass tolerance of 5 ppm for m/z < 250 and 3 ppm for higher masses. Clustered spectral features were organized into a table using an Excel macro. Background peaks were subsequently eliminated. The remaining peaks were assigned empirical formulas using the Formula Calculator v. 1.1 (http://magnet.fsu.edu/∼midas/download.html) and through the use of Kendrick diagrams.[30]

RESULTS AND DISCUSSION

Figure 1 shows high-resolution ESI mass spectra acquired in the positive mode for six BBA samples characterized in this study. The subsets of most abundant and metal-containing peaks are listed in Table 2. Mass spectra of BBA samples from different biomass produced markedly distinct peak patterns. Significant overlap between spectral features was observed only for L1, L2, and L10 samples collected at the same site. The similarity between mass spectra of the L samples suggests both that the ESI/HR-MS analysis has good reproducibility and that the variation in the BBA composition is due primarily to variation in the biomass.

The mass spectra of the VS, FB, L1, L2, and L10 samples contain several abundant peaks in common: $C_3H_8O_3Na^+$ (peak 16, m/z 115.037, glycerol), $C_6H_{10}O_5Na^+$ (peak 18, m/z 185.042, levoglucosan), and $C_{12}H_{24}O_3Na^+$ (peak 12, m/z 239.162, likely 2-methyl,3-hydroxypropanoic acid). The first two peaks are typical

Table 1. Types of Biomass Fuels Associated with WSOC-BBA Samples, Abbreviations, and Collection Sites

	fuel type	collection site
VM	manzanita	Vandenberg Air Force Base (VAFB), CA
VS	sage	Vandenberg Air Force Base (VAFB), CA
FB	pine	Fort Benning (FB), GA
L1	hardwood species, accumulation after 1 year	Marine Corps Base Camp Lejeune (MCBCL), NC
L2	hardwood species, accumulation after 2 years	Marine Corps Base Camp Lejeune (MCBCL), NC
L10	hardwood species, accumulation after 10+ years	Marine Corps Base Camp Lejeune (MCBCL), NC

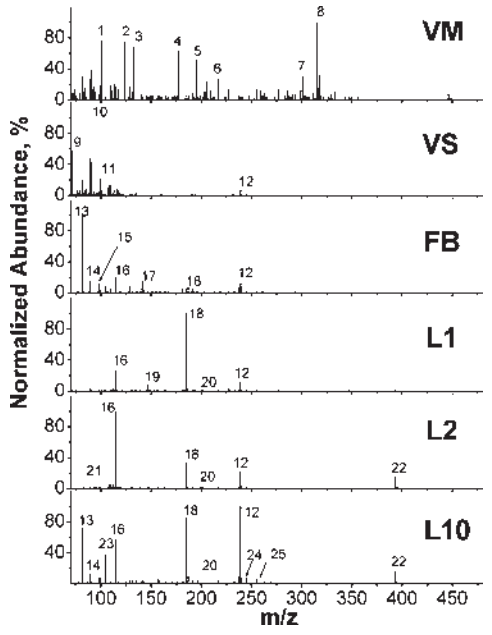

Figure 1. ESI (+) mass spectra of six different BBA extracts collected by PILS. The following peaks are labeled in the spectra: 1 - $C_4H_8N_2OH^+$; 2 - $C_6H_9N_3H^+$; 3 - $C_{10}H_{12}H^+$; 4 - $C_{13}H_{20}H^+$; 5 - $C_{13}H_{22}OH^+$; 6 - $C_{10}H_{16}O_5H^+$; 7 - $C_{19}H_{24}O_3H^+$; 8 - $C_{20}H_{26}O_3H^+$; 9 - CaO_2^+; 10 - unassigned (89.9625); 11 - $C_2H_3O_2Ca^+$; 12 - $C_{12}H_{24}O_3Na^+$; 13 - $C_2H_5NONa^+$; 14 - $C_2H_3NBa^{2+}$; 15 - $C_2H_3N_3O_4Zn^{2+}$; 16 - $C_3H_8O_3Na^+$; 17 - $C_4H_{10}N_2O_2Na^+$; 18 - $C_6H_{10}O_5Na^+$; 19 - Unassigned (147.0309); 20 - $C_6H_{10}O_6Na^+$; 21 - $C_3H_8O_2Na^+$; 22 - $C_{18}H_{16}O_{10}H^+$; 23 - $C_4H_6N_4O_3Cr^{2+}$; 24 - $C_{12}H_{14}O_4Na^+$; 25 - $C_{15}H_{20}O_2Na^+$. Additional peaks are listed in Table 2.

markers of BBA.[31] However, other previously detected BBA markers, such as benzoic acid and dehydroabietic acid,[31] were not observed in this study. The third abundant peak, $C_{12}H_{24}O_3Na^+$, has not been previously detected in BBA particles. It could potentially correspond to a high molecular weight (MW) product of nitroglycerine pyrolysis associated with military activities.[32] Other abundant features found in most of the samples examined in this study include $C_2H_3NBa^{2+}$ (m/z 89.4654), $C_2H_3N_3O_4Zn^{2+}$ (m/z 98.4707), and $C_3H_3O_3S_1Ca^+$ (m/z 217.067).

The mass spectra of VM and VS samples are remarkably different: both from each other and from the other samples. Abundant peaks unique for each fuel (peaks 1−8 in the VM sample and peaks 9−11 in the VS sample, respectively) were observed for these samples. The VM spectrum contains a number of protonated hydrocarbon species (e.g., $C_{10}H_{12}$ and $C_{13}H_{22}$) − molecules of low proton affinity that are rarely observed in ESI/MS. Several particularly abundant peaks correspond to metal-containing species.

There is only a small overlap (<10%) between high-resolution mass spectra obtained in this study and ESI/MS mass spectra of BBA reported in our previous studies.[18,19] As shown in Table 2, some overlap was found between organic constituents detected in this study and peaks found in BBA samples from laboratory burns of Alaskan duff (AD), Ponderosa pine duff (PPD), and dried southern pine needles (SPN) examined in our previous studies. In those studies ESI/MS spectra of BBA extracts were dominated by signals corresponding to protonated $[M+H]^+$ and sodiated $[M+Na]^+$ species.

Fewer than 30% of mass spectral features observed in this study could be identified assuming composition settings similar to our previous work: C (up to 100 atoms), H (up to 100 atoms), N (up to 4 atoms), O (up to 15 atoms), S (up to 1 atom), and Na (up to 1 atom). Table 2 lists the most abundant MS peaks that were successfully assigned to $[M+H]^+$ and $[M+Na]^+$ ions; where "M" indicates a neutral molecule. A number of sulfur-containing compounds were detected both as $[M+Na]^+$ species (e.g., $C_2H_5NOSNa^+$, m/z 113.9985) and as protonated molecules (e.g., $C_3H_7S^+$, m/z 75.0263; $C_3H_7N_2O_2S^+$, m/z 147.02206). Surprisingly, nearly 70% of abundant peaks remained unassigned using the original settings. More detailed analysis showed that a majority of the unidentified peaks correspond to metal- and phosphorus-containing organic compounds. None of these species were detected in our previous studies.[18,19]

Figure 2 shows the distribution of mass defect values for L1 and L10 samples (corresponding plots for all six samples are shown in Figure 1S of the Supporting Information). The mass defect is defined as a difference between the measured m/z and the nearest lower integer. The data provide an interesting insight on the possible elemental composition of the detected peaks. First, there is a significant fraction of peaks with mass defect exceeding 0.7 amu, which is characteristic for species containing sulfur, phosphorus, and metals. Second, in all the samples, there are also groups of peaks with mass defects between 0.4 and 0.6 amu corresponding to doubly charged ions, attributed to metal−organic species. The MW of compounds observed as doubly charged ions can be obtained by multiplying the measured value of m/z by a factor of 2. However, aside from the doubly charged species, it is difficult to identify metal-containing species based on the accurate mass measurement alone. Identification of metal-containing species is complicated for a number of reasons: 1) metals can assume different oxidation states; 2) organic molecules can be bound to metals as deprotonated species; and 3) metal-containing species can be found both as singly charged and multiply charged peaks in the same mass spectrum.

In this study, we use accurate mass measurement combined with calculated isotope distributions of candidate compounds to assign both singly- and doubly charged metal-containing species. Examples of calculated and experimental isotope distributions

Table 2. Subset of Most Abundant and Metal-Containing Peaks Observed in Positive ESI Spectra of WSOC-BBA Samples[a]

peak markers[b] in Figure 1	*m/z*	normalized abundance of peaks in WSOC-BBA samples listed in Table 1						elemental composition	charge state	observed in previous ESI/MS study[c]	tentative assignment
		VM	VS	FB	L1	L2	L10				
						Most Abundant Peaks					
	76.0394	15.5		3.9			1.3	$C_2H_6N_1O_2$	1		glycine
13	**82.0265**	6.2	35.2	100.0			72.1	**$C_2H_5N_1O_1Na$**	1	SPN	
	95.0856		12.6			3.0		C_7H_{11}	1		
21	**99.0418**		19.5	4.8		7.6	11.2	**$C_3H_8O_2Na$**	1		
1	**101.071**	76.2						**$C_4H_9N_2O_1$**	1		
	109.1013		22.4	0.1		5.8		C_8H_{13}	1		
16	115.0367		2.1	19.6	26.8	100.0	57.3	**$C_3H_8O_3Na$**	1	PPD/SPN	glycerol
2	**124.0869**	75.4						**$C_6H_{10}N_3$**	1		
3	**133.1012**	**69.2**						**$C_{10}H_{13}$**	**1**		
	140.959			6.2		0.8	4.2	$C_2H_6O_1S_2P_1$	1		
17	**141.0635**			15.0		0.0	1.2	**$C_4H_{10}N_2O_2Na$**	1		
19	**147.0309**				7.7	0.8	0.8	**unassigned**	1		
4	**177.164**	63.6						**$C_{13}H_{21}$**	1		
18	**185.0423**			6.2	100.0	33.5	84.7	**$C_6H_{10}O_5Na$**	1	All	levoglucosan
	185.115		1.1	5.1	1.7	1.6	7.5	$C_8H_{18}O_3Na$	1		
	191.1045		1.4	6.0	0.8	1.3	4.4	$C_{10}H_{16}O_2Na$	1	AD	methylcatechol
5	**195.1745**	51.6						**$C_{13}H_{23}O_1$**	1	AD	
20	**201.0371**			0.7	6.0	4.5	11.3	**$C_6H_{10}O_6Na$**	1		
6	**217.1072**	27.6						**$C_{10}H_{17}O_5$**	1		
12	**239.1619**		13.2	12.6	11.4	22.0	100.0	**$C_{12}H_{24}O_3Na$**	1		2-methyl,-3-hydroxy, propanoic acid
24	**245.0787**		1.4	1.0	1.0	1.4	7.7	**$C_{12}H_{14}O_4Na$**	1	AD	diethyl phthalate
25	**255.1359**		0.5	1.2	1.1	0.7	5.8	**$C_{15}H_{20}O_2Na$**	1	All	
7	**301.1802**	29.4				0.1		**$C_{19}H_{25}O_3$**			
8	**315.1957**	100.0				0.3		**$C_{20}H_{27}O_3$**	1	AD	
22	**393.0832**		0.9	0.4	0.6	14.7	16.8	**$C_{18}H_{17}O_{10}$**	1	PPD/AD	
						Metal-Containing Peaks					
	70.0127	20.2		0.1				$C_4H_8N_2O_1Ca$	2		
9	**71.9521**		100.0	0.5	0.9	0.1	0.3	**CaO_2**	**1**		
	72.9907	9.4						$C_4H_6N_2Zn$	2		methylimidazole
	76.4704		12.5					$(CH_2NH{+}H_4P_2)Ni$	2		
	78.9991	4.4	11.1	0.3				$C_4H_7O_3P_1Mg$	2		
	83.9969	4.4	11.9	0.3				$C_4H_6N_4Ni$	2		
	84.9599		14.7	0.1	0.2			$C_1H_1O_2Ca$	1		
	85.4756		7.2					$C_2H_5N_1O_4Zn$	2		hydroxyethyl nitrate
14	**89.4654**	27.3	80.3	15.6	2.6	1.6	13.4	**C_2H_3NBa**	2		acetonitrile
10	**89.9625**		100.00	0.9	2.7	0.2	0.7	**unassigned**			
	90.507	39.0	71.0				3.1	$C_6H_9N_3Ni$	2		
15	**98.4707**	3.2	7.8	12.2	0.4	0.6	4.3	**$C_2H_3N_3O_4Zn$**	2		
11	**98.9754**		37.4	0.9	0.6		6.1	**$C_2H_3O_2Ca$**	1	PPD	acetic acid
	99.5123	17.9					1.7	$C_6H_{11}N_3O_1Ni$	2		
	100.51	4.7	11.6				0.5	$C_5H_{11}N_3O_2Fe$	2		
23	**104.9923**			19.8	0.2	0.2	15.7	**$C_4H_6N_4O_3Cr$**	2		
	109.9787	18.2	18.8	4.8			2.6	$C_6H_4N_2O_4Cr$	2		dinitrobenzene
	112.9785		14.1					$C_1H_4N_3Mn$	1		
	115.9642		13.1				0.1	$C_2H_4N_1O_1Ni$	1		acetamide
	116.9859		10.7	0.4			4.0	$C_2H_5O_3Ca$	1	SPN	
	118.9838		1.4	3.1				$C_7H_6N_2O_4Fe$	1		dinitrotoluene
	127.9892			2.4			0.1	$C_6H_3N_3O_7Al$	2		picric acid
	186.9955			7.0			10.3	$C_9H_8O_1Mn$	1		

[a] Extended list of these peaks is also presented in Table S1 of the Supporting Information. [b] Peaks labeled in Figure 1 and listed in Table 2 are highlighted in bold. [c] Peaks observed in ESI/MS spectra are reported in refs 18 and 19. Acronyms used in this column denote BBA samples collected during laboratory burns of the following biomass fuels: AD - Alaskan Duff, PPNS - Ponderosa Pine Needles and Sticks, PPD - Ponderosa Pine Duff, SPN - Dried southern pine needles, - SCC Southern California ceanothus.

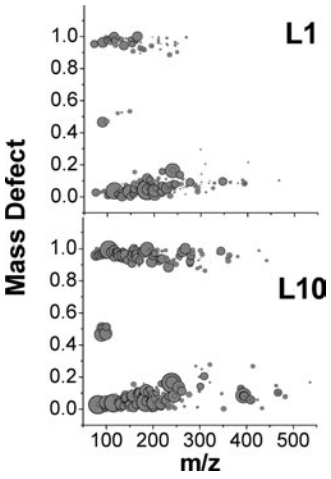

Figure 2. Mass defect values of individual MS peaks detected in L1 and L10 samples of WSOC-BBA. The size of the points is proportional to peak intensities. Legends as to fuel source and type are from Table 1. Corresponding plots for all six samples are shown in Figure S1 of the Supporting Information.

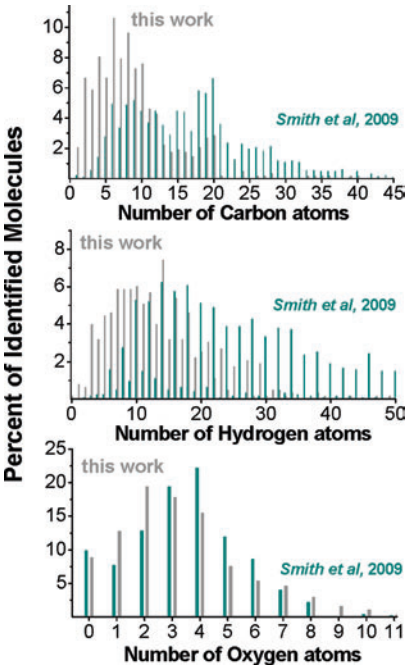

Figure 3. Distributions of the number of C, H, and O atoms in identified species observed in all samples conveyed in this work, as compared to our previous studies.[18,19].

are shown in Figure S2 of the Supporting Information. Typical settings used for identification of organic cores are as follows: C (up to 100 atoms), H (up to 100 atoms), N (up to 10 atoms), O (up to 20 atoms), S (up to 2 atoms), and P (up to 1 atom). The mass measurement error was lower than 0.0006 amu. Elemental compositions and charge states of metal-containing peaks are listed in Table 2. All doubly charged species correspond to metal ions in the +2 oxidation state bound to neutral organic molecules, while singly charged ions correspond to deprotonated molecules bound to metal dications. For example, the composition of $C_2H_3O_2Ca^+$ at m/z 98.9754 is described as $[C_2H_3O_2-H]^-+Ca^{2+}$, while $C_2H_3NBa^{2+}$ at m/z 89.4654 corresponds to a neutral C_2H_3N bound to Ba^{2+}. Organic compounds containing Cr^{2+}, Fe^{2+}, Ni^{2+}, Cu^{2+}, Zn^{2+}, Mn^{2+}, Mg^{2+}, and Ba^{2+} were assigned empirical formulas using this approach. In addition, a number of small molecules cationized on calcium were also identified. Observation of abundant metal-containing peaks is quite surprising because ESI is not particularly sensitive to transition metal cations.

Species containing rare earth and transition metals were detected in all six BBA samples. However, the corresponding organic counterparts varied between the samples with only a few common peaks found for all the samples. A variety of calcium-containing species were observed in the VS sample. Calcium is predominantly bound to small oxygenated organic molecules. Its source is not directly known but may be related to mineral dust deposited on the plants. Energetic organic compounds including picric acid, dinitrobenzene, and dinitrotoluene were also observed in conjunction with metal cations. These compounds are characterized by high O/C and N/C ratios.

Similarity between the L1, L2, and L10 samples produced by burning the hardwood vegetation collected at the same base (Lejeune) indicate buildup of the metal−organic species over consecutive years of regrowth. This may be from uptake of metals associated with military use or nearby industries. While further study is needed, metal accumulation by plants may explain these results. An additional source of metal−organic compounds in BBA may be the resuspension during burning events of previous MCA deposits on surfaces of plants. Regardless of the exact mechanism, our results indicate that water-soluble metal−organic compounds can be aerosolized during biomass burning and have the potential for long-range transport.

We note that spectra obtained in this study have 30−60% fewer peaks than in our previous ESI/HR-MS analysis of BBA samples collected on substrates and extracted in organic solvents.[18,19] The smaller number of peaks is attributed to poor solubility in water of the medium- to higher-MW (400−700 g/mol) BBA organic compounds. Recent study has demonstrated that a significant fraction of higher-MW compounds are more efficiently extracted into organic solvents.[20]

Figure 3 shows the distributions of the number of C, H, and O atoms in the constituents of the six BBA samples examined in this study as compared to those of the BBA samples from previous studies.[18,19] The BBA samples of this study are mainly composed of relatively small organic molecules containing 2−15 carbon atoms, while heavier molecules of 5−30 carbon atoms were detected in our previous studies.

Distributions of H atoms are also different in two cases. The distribution of H atoms in BBA constituents detected in this study is quite uniform and contains both even and odd numbers. In contrast, samples examined in our previous work contain molecules with mostly an even number of H atoms distributed over a wider range (6−50 H atoms). The observations indicate the presence of a CH_2-based series of homologous organic compounds observed in previous works, while relatively small molecules without homologues were typical for the BBA samples in the present work.

Distributions of O atoms are very similar for all the BBA constituents we have studied to date, with 2−5 oxygen atoms present in individual molecules. However, because of the lower carbon content, the extent of oxygenation is substantially higher for BBA constituents detected in this study. This is further exemplified in Figure 4, which shows Van Krevelen plots obtained for the samples examined here in comparison with the data from our previous studies.[18,19] A significant number of highly oxidized species is clearly present in all the samples with average O/C

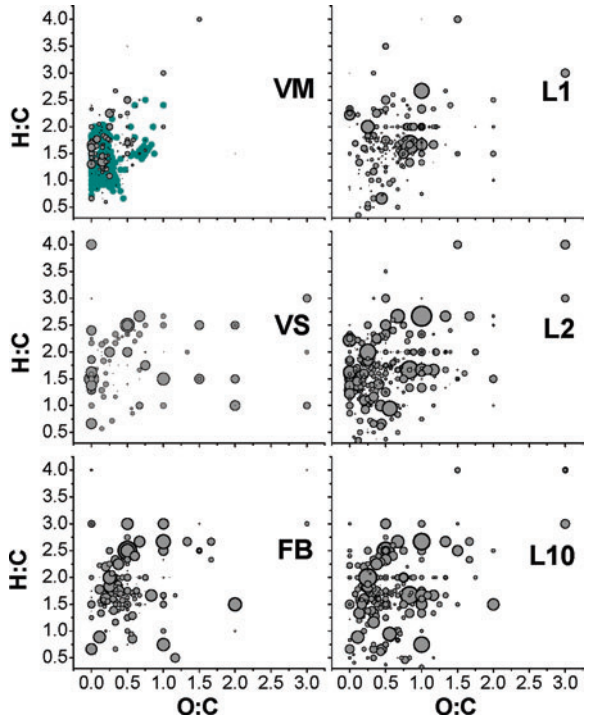

Figure 4. van K revelen plot of H:C versus O:C atomic ratios for species identified in six WSOC-BBA samples. The plot provides a visual representation of the degree of oxidation of the identified species. The size of the points is proportional to the peak intensities. The data correspond to neutral species inferred from positive ESI mass spectra. Cyan points in the upper left panel show Ponderosa pine needles and sticks (PPNS) data from our previous studies [18,19] for comparison. Legends as to fuel source and type are from Table 1.

ratios close to unity. In contrast, O/C ratios obtained in our previous work were lower by approximately a factor of 2, indicative of less oxygenated, larger size organic molecules as can be inferred from both Figures 3 and 4.

The higher average O/C ratio for the organic constituents of BBA detected in this study might be due to different combustion conditions, different analysis approaches, or different land use effects that could result in the presence of energetic compounds from military activities. Previous study compared the O/C ratios obtained from ESI/HR-MS analysis of BBA samples collected by PILS and samples produced from burning of the same biomass fuel extracted from substrates into organic solvents.[20] HR-MS spectra observed in that study were dominated by compounds containing C, H, N, O, and Na; metal-containing compounds were not observed. Somewhat higher averaged O/C ratio observed for PILS samples (0.29) as compared to organic solvent extracts (0.19) was attributed to reduced solubility of higher-MW BBA constituents in water. In contrast, energetic metal-containing species are possibly main contributors to the high O/C ratios observed in this study (see Table 2). Explosives and their degradation products have been found as groundwater contaminants at military sites.[13,33] These compounds may be accumulated in the biomass material. For example, dinitrotoluene is readily dissolved in water and is stable toward biochemical oxidation and hydrolysis under environmental conditions. Similarly, picric acid does not degrade biochemically and is produced as a result of slow hydrolysis of other explosive compounds. Such compounds may disperse through the ecosystem and end up in, or on, the biomass.

In summary, we have observed metal-containing WSOC compounds in the BBA samples produced by burns of biomass collected from sites managed by prescribed fire. These compounds could be accumulated in, or deposited on, the biomass and transferred into BBA. Thus, biomass burning may be a source of aerosols with water-soluble N-, S-, P-, and metal-containing organic species that could be subsequently transported over significant distances. Further investigations are needed to determine how site vegetation, location, usage history, and sampling techniques affect the detected levels of these compounds and to assess the fate of these species in the environment. Additional research is needed to quantify both the emissions and the ambient concentrations of airborne metal-containing WSOC/N and determine the relative impact of uptake from soils and dry deposition of MCA in enhancing their re-emissions. Further understanding of these factors could potentially lead to successful mitigation strategies.

■ ASSOCIATED CONTENT

Supporting Information. Figures S1 and S2 and Table S1. This material is available free of charge via the Internet at http://pubs.acs.org.

■ AUTHOR INFORMATION

Corresponding Author

*E-mail: Alexander.Laskin@pnl.gov (A.L.), Julia.Laskin@pnl.gov (J.L.).

■ ACKNOWLEDGMENT

ESI/HRMS analysis was performed at the W. R. Wiley Environmental Molecular Sciences Laboratory (EMSL), a national scientific user facility sponsored by the U.S. Department of Energy (DOE), Office of Biological and Environmental Research and located at Pacific Northwest National Laboratory (PNNL). PNNL is operated by Battelle for the U.S. DOE. The authors acknowledge support from the Chemical Sciences Division, Office of Basic Energy Sciences of the U.S. DOE (J.L.); the intramural research and development program of EMSL (A.L); the DOE Science Undergraduate Laboratory Internship (SULI) program (A.C.-G.); the Strategic Environmental Research and Development Program (SERDP), project SI-1649 (L.T.M.P., T. J.J., and R.J.Y.). The authors gratefully acknowledge the staff at the USDA/USFS Fire Sciences Laboratory for technical help during sample collection.

■ REFERENCES

(1) Bond, T. C.; Streets, D. G.; Yarber, K. F.; Nelson, S. M.; Woo, J.-H.; Klimont, Z. A technology-based global inventory of black and organic carbon emissions from combustion. *J. Geophys. Res., [Atmos.]* **2004**, *109*, D14203.

(2) Kundu, S.; Kawamura, K.; Andreae, T. W.; Hoffer, A.; Andreae, M. O. Diurnal variation in the water-soluble inorganic ions, organic carbon and isotopic compositions of total carbon and nitrogen in biomass burning aerosols from the LBA-SMOCC campaign in Rondonia, Brazil. *J. Aerosol Sci.* **2010**, *41* (1), 118–133.

(3) Martin, S. T.; Andreae, M. O.; Artaxo, P.; Baumgardner, D.; Chen, Q.; Goldstein, A. H.; Guenther, A.; Heald, C. L.; Mayol-Bracero, O. L.; McMurry, P. H.; Pauliquevis, T.; Poschl, U.; Prather, K. A.; Roberts, G. C.; Saleska, S. R.; Dias, M. A. S.; Spracklen, D. V.; Swietlicki, E.; Trebs, I. Sources and Properties of Amazonian Aerosol Particles. *Rev. Geophys.* **2010**, *48*, RG2002.

(4) Dinar, E.; Anttila, T.; Rudich, Y. CCN activity and hygroscopic growth of organic aerosols following reactive uptake of ammonia. *Environ. Sci. Technol.* **2008**, *42* (3), 793–799.

(5) Dinar, E.; Taraniuk, I.; Graber, E. R.; Katsman, S.; Moise, T.; Anttila, T.; Mentel, T. F.; Rudich, Y. Cloud Condensation Nuclei properties of model and atmospheric HULIS. *Atmos. Chem. Phys.* **2006**, *6*, 2465–2481.

(6) Facchini, M. C.; Mircea, M.; Fuzzi, S.; Charlson, R. J. Cloud albedo enhancement by surface-active organic solutes in growing droplets. *Nature* **1999**, *401* (6750), 257–259.

(7) Andreae, M. O.; Gelencser, A. Black carbon or brown carbon? The nature of light-absorbing carbonaceous aerosols. *Atmos. Chem. Phys.* **2006**, *6*, 3131–3148.

(8) Chen, Y.; Bond, T. C. Light absorption by organic carbon from wood combustion. *Atmos. Chem. Phys.* **2010**, *10* (4), 1773–1787.

(9) Jurado, E.; Dachs, J.; Duarte, C. M.; Simo, R. Atmospheric deposition of organic and black carbon to the global oceans. *Atmos. Environ.* **2008**, *42*, 7931–7939.

(10) Cornell, S. E.; Jickells, T. D.; Cape, J. N.; Rowland, A. P.; Duce, R. A. Organic nitrogen deposition on land and coastal environments: a review of methods and data. *Atmos. Environ.* **2003**, *37* (16), 2173–2191.

(11) Vasconcellos, P. C.; Balasubramanian, R.; Bruns, R. E.; Sanchez-Ccoyllo, O.; Andrade, M. F.; Flues, M. Water-soluble ions and trace metals in airborne particles over urban areas of the state of sauo paulo, Brazil: Influences of local sources and long range transport. *Water, Air, Soil Pollut.* **2007**, *186* (1−4), 63–73.

(12) Moffet, R. C.; Desyaterik, Y.; Hopkins, R. J.; Tivanski, A. V.; Gilles, M. K.; Wang, Y.; Shutthanandan, V.; Molina, L. T.; Abraham, R. G.; Johnson, K. S.; Mugica, V.; Molina, M. J.; Laskin, A.; Prather, K. A. Characterization of aerosols containing Zn, Pb, and Cl from an industrial region of Mexico City. *Environ. Sci. Technol.* **2008**, *42* (19), 7091–7097.

(13) Berthelot, Y.; Valton, E.; Auroy, A.; Trottier, B.; Robidoux, P. Y. Integration of toxicological and chemical tools to assess the bioavailability of metals and energetic compounds in contaminated soils. *Chemosphere* **2008**, *74* (1), 166–177.

(14) Mingorance, M. D.; Valdes, B.; Oliva, S. R. Strategies of heavy metal uptake by plants growing under industrial emissions. *Environ. Int.* **2007**, *33* (4), 514–520.

(15) Oliva, S. R.; Mingorance, M. D. Assessment of airborne heavy metal pollution by aboveground plant parts. *Chemosphere* **2006**, *65* (2), 177–182.

(16) Deguillaume, L.; Leriche, M.; Desboeufs, K.; Mailhot, G.; George, C.; Chaumerliac, N. Transition metals in atmospheric liquid phases: Sources, reactivity, and sensitive parameters. *Chem. Rev.* **2005**, *105* (9), 3388–3431.

(17) Reemtsma, T. Determination of molecular formulas of natural organic matter molecules by (ultra-) high-resolution mass spectrometry Status and needs. *J. Chromatogr., A* **2009**, *1216* (18), 3687–3701.

(18) Laskin, A.; Smith, J. S.; Laskin, J. Molecular characterization of nitrogen-containing compounds in biomass burning aerosols using high-resolution mass spectrometry. *Environ. Sci. Technol.* **2009**, *43*, 3764–3771.

(19) Smith, J. S.; Laskin, A.; Laskin, J. Molecular characterization of biomass burning aerosols using high-resolution mass spectrometry. *Anal. Chem.* **2009**, *81*, 1512–1521.

(20) Bateman, A. P.; Nizkorodov, S. A.; Laskin, J.; Laskin, A. High-Resolution Electrospray Ionization Mass Spectrometry Analysis of Water Soluble Organic Aerosols Collected with a Particle into Liquid Sampler (PILS). *Anal. Chem.* **2010**, *82*, 8010–8016.

(21) Weber, R. J.; Orsini, D.; Daun, Y.; Lee, Y.-N.; Klotz, P. J.; Brechtel, R. A particle-into-liquid collector for rapid measurement of aerosol bulk chemical composition. *Aerosol Sci. Technol.* **2001**, *35*, 718–727.

(22) Song, C. H.; Ma, Y.; Orsini, D.; Kim, Y. P.; Weber, R. J. An investigation into the ionic chemical composition and mixing state of biomass burning particles recorded during TRACE-P P3B Flight#10. *J. Atmos. Chem.* **2005**, *51* (1), 43–64.

(23) Miyazaki, Y.; Kondo, Y.; Shiraiwa, M.; Takegawa, N.; Miyakawa, T.; Han, S.; Kita, K.; Hu, M.; Deng, Z. Q.; Zhao, Y.; Sugimoto, N.; Blake, D. R.; Weber, R. J. Chemical characterization of water-soluble organic carbon aerosols at a rural site in the Pearl River Delta, China, in the summer of 2006. *J. Geophys. Res., [Atmos.]* **2009**, *114*, D14208.

(24) Peltier, R. E.; Weber, R. J.; Sullivan, A. P. Investigating a liquid-based method for online organic carbon detection in atmospheric particles. *Aerosol Sci. Technol.* **2007**, *41* (12), 1117–1127.

(25) Parshintsev, J.; Rasanen, R.; Hartonen, K.; Kulmala, M.; Riekkola, M. L. Analysis of organic compounds in ambient aerosols collected with the particle-into-liquid sampler. *Boreal Environ. Res.* **2009**, *14* (4), 630–640.

(26) Lee, S.; Baumann, K.; Schauer, J. J.; Sheesley, R. J.; Naeher, L. P.; Meinardi, S.; Blake, D. R.; Edgerton, E. S.; Russell, A. G.; Clements, M. Gaseous and particulate emissions from prescribed burning in Georgia. *Environ. Sci. Technol.* **2005**, *39* (23), 9049–9056.

(27) Oakes, M.; Rastogi, N.; Majestic, B. J.; Shafer, M.; Schauer, J. J.; Edgerton, E. S.; Weber, R. J. Characterization of soluble iron in urban aerosols using near-real time data. *J. Geophys. Res., [Atmos.]* **2010**, *115*, D15302.

(28) Burling, I. R.; Yokelson, R. J.; Griffith, D. W. T.; Johnson, T. J.; Veres, P.; Roberts, J. M.; Warneke, C.; Urbanski, S. P.; Reardon, J.; Weise, D. R.; Hao, W. M.; de Gouw, J. Laboratory measurements of trace gas emissions from biomass burning of fuel types from the Southeastern and Southwestern United States. *Atmos. Chem. Phys. Discuss.* **2010**, *10*, 16425–16473.

(29) Hopkins, R. J.; Lewis, K.; Desyaterik, Y.; Wang, Z.; Tivanski, A. V.; Arnott, W. P.; Laskin, A.; Gilles, M. K. Correlations between optical, chemical and physical properties of biomass burn aerosols. *Geophys. Res. Lett.* **2007**, *34* (18), L18806.

(30) Kendrick, E.; Mass, A Scale Based on CH2=14.0000 for High Resolution Mass Spectrometry of Organic Compounds. *Anal. Chem.* **1963**, *35* (13), 2146–&.

(31) Simoneit, B. R. T. Biomass burning - A review of organic tracers for smoke from incomplete combustion. *Appl. Geochem.* **2002**, *17* (3), 129–162.

(32) Cropek, D. M.; Kemme, P. A.; Day, J. M. *Pyrolytic Decomposition Studies of AA2, A Double-Base Propellant*; technical report, ERDC/CERL TR-01-66; Construction Engineering Research Laboratory: **2001**.

(33) Clausen, J.; Robb, J.; Curry, D.; Korte, N. A case study of contaminants on military ranges: Camp Edwards, Massachusetts, USA. *Environ. Pollut.* **2004**, *129* (1), 13–21.